Method of diagnostics of the short-circuited rotor damage on point induction converters

Cite as: AIP Conference Proceedings **2337**, 030001 (2021); https://doi.org/10.1063/5.0046565
Published Online: 08 March 2021

Oxana Andreyeva, Alexandr Neftissov, and Alena Mileiko

Method of Diagnostics of the Short-Circuited Rotor Damage on Point Induction Converters

Oxana Andreyeva[1, a)], Alexandr Neftissov[1] and Alena Mileiko[2, b)]

[1]*Toraighyrov University, 140000, Pavlodar, Kazakhstan.*
[2]*Novosibirsk State University, 630090, Novosibirsk, Russia.*

[a)]Corresponding author: andreyeva.oa@mail.ru
[b)]alena.mileyko@mail.ru

Abstract. A method has been developed for diagnostics of the short-circuited rotor damage of asynchronous motor by external magnetic field. The information sign is a change in amplitude of harmonic components of this field measured with the help of point induction converters. A method for determining the sliding of an asynchronous motor by an external magnetic field is proposed.

INTRODUCTION

The external magnetic field (EMF) of an asynchronous motor (AM) contains informative harmonic components, the frequencies of which depend on the network frequency f_1, sliding s and the number of pairs of poles p. Knowing these parameters, you can find any harmonic generated by AM [1, 2].

In this paper it is proposed to obtain information about the damage of the "squirrel cell" from the EMF by means of point induction converters (PIC) placed inside or outside the AM. The implementation of the method of diagnostics of damage to the short-circuited rotor with a reed involves some difficulties. Firstly, a temporary installation of the slip measurement sensor for each motor to be diagnosed is necessary. Secondly, the sensitivity of the diagnostic device is sometimes insufficient to detect damage in the “squirrel cage” [3-4].

If the air gap scattering field is neglected, then EMF in PIC, which is located in the end zone or outside, induced only by the currents of the stator and rotor windings. In this case, according to [2], the rotor winding currents are represented as undamaged rotor currents and additional currents. The range of components of this EMF PIC depends on its location, design features of the AM and the state of its “squirrel cage”, mode of operation and type of load [5-7]. Information on the damage of a “squirrel cell” necessary for further studies can be one or more harmonic of this spectrum in the frequency range 0-50 Hz, which is divided into $i = (p-1)$ measurement areas.

The currents I_1 flowing in the stator winding with a network frequency $f_1 = 50$ Hz, form in the front-end of the AM magnetic fluxes of frontal scattering and induce in the windings of EMF PIC with a network frequency. Its amplitude value can be defined as:

$$E_{n1} = 2\pi f_1 B_{z1} S_n w_n \tag{1}$$

Where B_{z1} is induction of the magnetic field of the stator winding frontal scattering, crossing the PIC plane; S_n is PIC area, w_n is number of PIC coil turns.

Short-circuited rotor AM winding forms magnetic field of frontal scattering with number of poles equal p, rotating with angular speed $\omega_2 = \omega_1 / p$ relative to PIC and induces in it EMF with amplitude value:

Thermophysical Basis of Energy Technologies (TBET 2020)
AIP Conf. Proc. 2337, 030001-1–030001-5; https://doi.org/10.1063/5.0046565
Published by AIP Publishing. 978-0-7354-4081-4/$30.00

$$E_{n2} = 2\pi \frac{f_1}{p} B_{z2} S_n w_n \tag{2}$$

Where B_{z2} is induction of the magnetic field of the frontal scattering of the whole rotor winding, crossing the plane PIC.

At the same time, the field of frontal scattering from the current of the damaged element of the short-circuited winding rotor AM has one pair of poles and rotates with an angular velocity $\omega_{2_r} = \omega_1 / p(1-s)$ relative to the PIC and induces in it an EMF:

$$E_{n2e} = 2\pi \frac{f_1}{p} (1-s) B_{z2e} S_n w_n \tag{3}$$

Where B_{z2e} is induction of magnetic field of frontal scattering from additional current in elements of short-circuit ring at rotor rod break.

Nonlinearity of dependence $B_{z2e} = f(x)$ and load, and consequently uneven rotor sliding, cause the appearance of additional harmonic EMFs, which is determined how to:

$$E_{n2\partial} = 2\pi \frac{f_1}{p} \left[(1-s) \pm nsp\right] B_{z2e} S_n w_n, \; n = 1; 3; 5\ldots, \tag{4}$$

$$E^*_{n2\partial} = 2\pi \frac{f_1}{p} (1 \pm 2ksp) B_{n2e} S_n w_n, \; k = 1; 2; 3\ldots \tag{5}$$

EXPERIMENTAL INVESTIGATION

The analysis of the influence of rotor winding breaks and operational factors (voltage unbalance, static and dynamic eccentricity, load on the rotor shaft) changing within the permissible limits on the EMF spectrum has shown that as a diagnostic parameter of the presence of rotor breaks it is advisable to use a change in the amplitude of harmonic with frequencies $\left[(1-s) \mp ps\right] f_1 / p$ in the i – measurement area, or their ratio to the main harmonic of the network with a frequency f_1 in the form of coefficients K_u at a given rotor slip s.

Since the calculations require knowledge of the current value of rotor sliding, it can be calculated from some harmonic components of the magnetic field of air gap AM. To do this, it is necessary to determine in the area of displacement in accordance with Fig. 1 on the PIC EMF spectrum the parameters of harmonic EMFs with frequencies $f_1 / p\left[(1-s) \mp ps\right]$ that have the largest amplitudes in this area. The zone of displacement in this spectrum is limited by frequencies $f_1 / p\left[(1-s_n) \mp ps_n\right]$, where s_n – the nominal sliding of the AM rotor according to the passport data. The difference between these frequencies and the sliding will be equal to:

$$\Delta f_b = \frac{f_1}{p} \left[(1-s) + ps)\right] - \frac{f_1}{p} \left[(1-s) - ps)\right] = f_1 / p \; 2s \text{ and } s = \frac{p\Delta f_b}{2 f_1}. \tag{6}$$

It is easy to double the sensitivity by using two PICes. This method is distinguished by the fact that with the help of diametrically arranged and switched on counter PIC is measured not the external multipole field AM, and the external field AM with $2p = 2$.

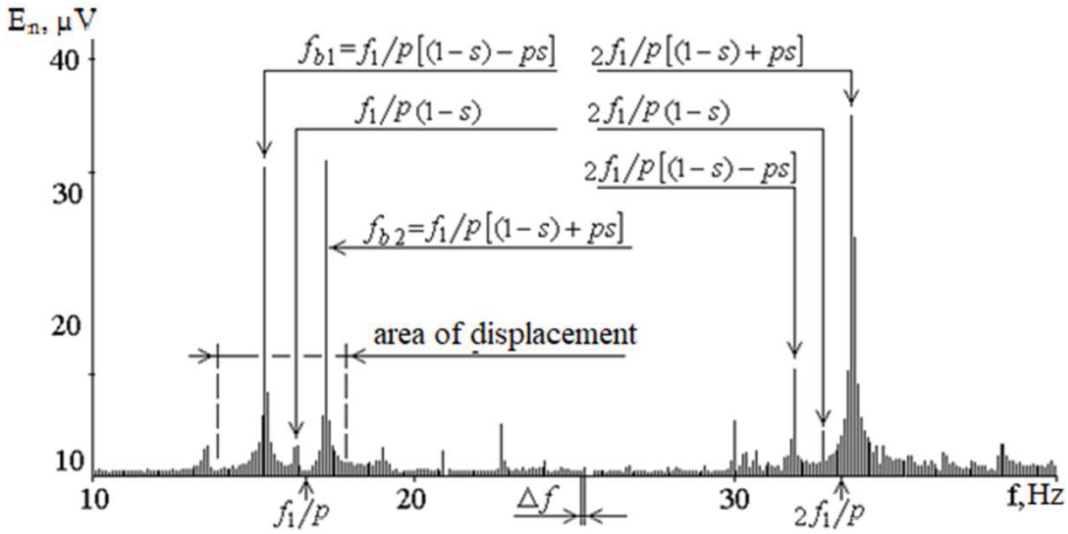

FIGURE 1. The fragment of the harmonic spectrum of EMF PIC at motor type 4AM100L6U3

Diagnostics damage of "squirrel cell" is carried out as follows. Initially, according to Fig. 2, during the time t_{e1} signal of one PIC is measured and during the time t_{e2} signal from the switched on counter PIC. Then, a signal from first PIC by decomposition in a series of Fourier E_{n1} EMF of the main harmonic network with a frequency f_1, and a signal from two PICes is EMF with frequencies $f_1/p\left[(1-s)\mp ps\right]$ [8-10].

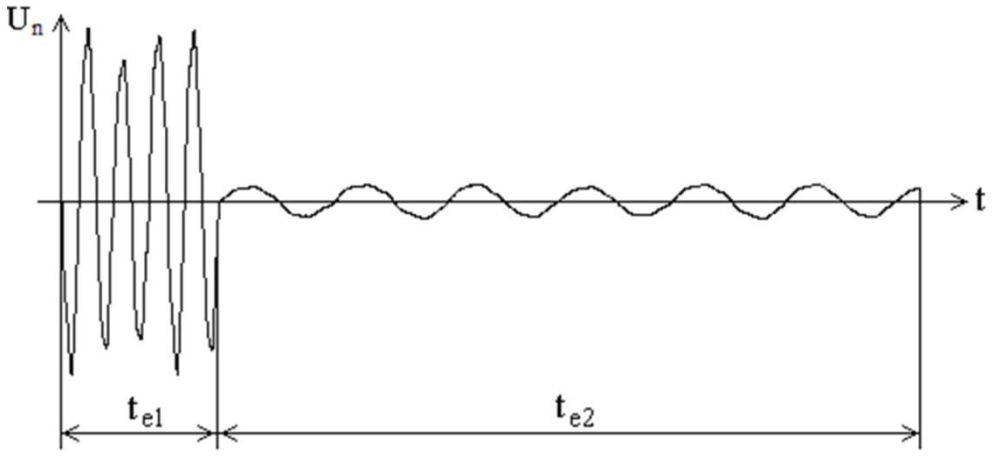

FIGURE 2. Oscillogram at the output of a measuring probe with two PICs in the diagnosis of "squirrel cell"

They are used to determine the slip by the parameters of harmonic EMFs with frequencies $f_1/p\left[(1-s)\pm ps\right]$ and the current value of the coefficient $K_u^* = (E_{n2\partial 1} + E_{n2\partial 2})/(\dot{E}_{n1} + \dot{E}_{n2})$. In the threshold element K_u^* it is compared with the threshold of triggering $K_{u\,tr}$ at the obtained slip. In case $K_u^* < K_{u\,tr}$, the display indication will give the information "ROTOR STAYED INTACT". In case $K_{u\,tr} < K_u^* < K_{u\,\max}$, the display indication will give the information "PARTICULARLY BREAKAGE OF ROD". If $K_u^* > K_{u\,\max}$, the display indication will show "BREAKAGE OF ROD".

In Fig. 3 shows a block diagram of this device, where PICes 1 and 2, AM 3 are connected to block of balancing these PIC EMF 4 and further to the first input 5 of block of switching 6. The second input 7 block of switching 6 is connected to the block of time 8. Output of the block of switching 6 through a block of memory 9 connected to the

block of decomposition 10 of the EMF of the PIC to harmonic components. Block 10 in turn connected to the block definition slip and coefficient $K_{u\,tr}$ 11. Output of block 11 through the threshold element 12 is connected to the block indication 13. The operation of block 6 is controlled by the time unit 8, which starts the diagnostic unit with key 14. Switching on and off the machine from the network is carried out by switch 15. Blocks 4, 6, 8 and 9 are located on the measuring dipstick, the rest are implemented through the computer [11-14].

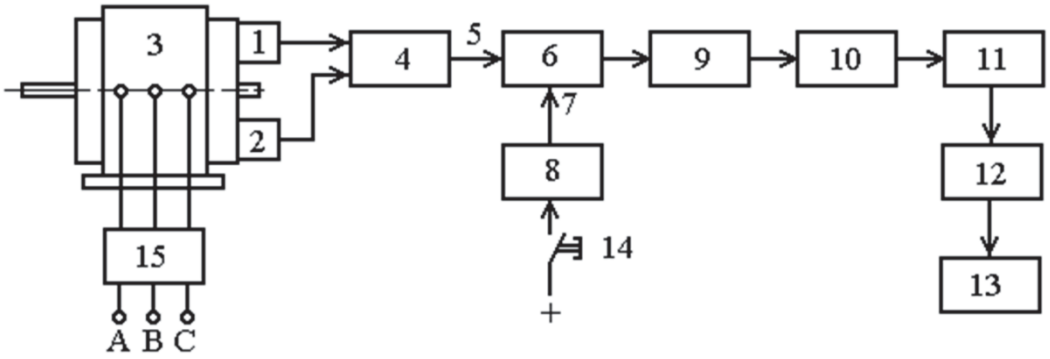

FIGURE 3. Block diagram of the device, which implements the method of "squirrel cell" damage diagnostics on PIC

Since the diametrically arranged PICes have a different number of turns and are inaccurately determined, and the AM has on the outside surface of various asymmetrical ferromagnetic elements, the EMF of these PICes from the external magnetic fields are not equal in value. To addressing this deficiency, the balancing unit 4 is used. One of the variants of its simplified scheme is shown in Fig. 4.

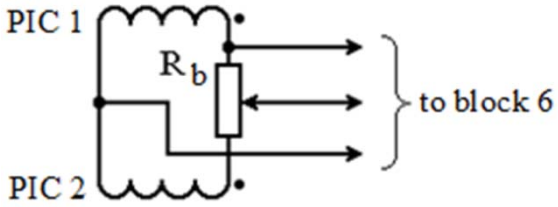

FIGURE 4. Simplified scheme of balancing block

Block 6 of switching is made in the form of electromagnetic relay, which is managed with the time relay. To the second input of 7 block 6 switching unit 8 time is connected. Its main task is to ensure the timely delivery of signals from one and two PICs to the input of block 9, in which they are recorded. The recording time, according to Fig. 2, is determined by the values t_{e1} and t_{e2}.

Recording the EMF signal from one PIC is used to determine the value of the main harmonic network with frequency f_1. Ideally, the time t_{e1} equal to one network period is sufficient for this. In fact, due to fluctuations in the amplitude of the PIC EMF, caused by various reasons, recording time t_{e1} should be taken equal to 0.1 – 0.5 s.

EMF from each of the PICs induced by the magnetic fields of the stator, rotor and damaged rod, taking into account equations (4) and (5) are equal, respectively:

$$E_{mun1} = 2\pi f_1 \left\{ B_{z1} + \frac{1}{p} B_{z2} + \frac{1}{p} B_{z2э} \left[(1-s) \pm ksp \right] \right\} s_n w_n;$$
$$E_{mun2} = 2\pi f_1 \left\{ B_{z1} + \frac{1}{p} B_{z2} - \frac{1}{p} B_{z2э} \left[(1-s) \pm ksp \right] \right\} s_n w_n \quad (7)$$

For diametrically arranged PICes, the windings of which are connected counter-sessionally, the resulting EMF is determined as the sum of their EMF. As a result:

$$E_{en2} = 2\pi f_1 \left\{ \frac{2}{p} B_{z2э} \left[(1-s) \pm ksp \right] \right\} s_n w_n \tag{8}$$

That is, under ideal conditions the resulting EMF will have no EMF from the magnetic fields of the stator and rotor. At the same time, the EMF from the damaged rod field will double. In this way, the sensitivity of the device increases significantly. It should be added that such switching allows almost complete adjustment from external magnetic fields.

The slip is determined by the frequency of two harmonic EMFs of the highest value in the area of movement. $f_1 / p\left[(1-s) \pm ps)\right]$.

CONCLUSION

The method has been developed for determining the Theoretical and experimental studies have shown that the spectrum of PIC EMF in the frequency range from 0 to f_1 broken down into $(p-1)$ measurement areas. The frequencies and amplitudes of additional harmonic $E_{n2\partial}$ which are most variable when the rods are damaged and do not depend on the unevenness of the load.

As a criterion for the serviceability of the AM rotor can be used as a change in the amplitude of the harmonic with frequencies $\left[(1-s) \mp ps\right] if_1 / p$ in the i – measurement areas, and their ratio to the main harmonic network with a frequency f_1 in the form of coefficient K_u^*.

In case implementing the method of diagnosis of damage the "squirrel cell" on point induction transducers rotor slip is determined by the difference of harmonics with frequencies $\left[(1-s) \mp ps\right] f_1 / p$.

REFERENCES

1. P. Tavner, *Condition Monitoring of Rotating Electrical Machines* (The Inst. of Eng. and Tech., 2008), p. 543.
2. O. A. Andreeva, Ph.D. thesis, Siberian State University of Water Transport, Novosibirsk, 2009 [in Russian].
3. M. Kletsel, N. Kabdualiyev, B. Mashrapov, and A. Neftissov, Prz. Elektrotech. **1**, 88–89 (2014).
4. A. B. Zhantlesova, M. Y. Kletsel, P. N. Maishev, and A. V. Neftisov, Russ. Electr. Eng. **85** (4), 210–216 (2014).
5. A. Novozhilov, Y. Kryukova, A. Kislov, O. Andreyeva, and T. Novozhilov, Life Sci. Journal, **11** (7), 502–505 (2014).
6. A. Novozhilov, Y. Kryukova, A. Kislov, O. Andreyeva, and T. Novozhilov, Life Sci. Journal, **11** (8), 116–119 (2014).
7. A. Novozhilov, Y. Kryukova, O. Andreyeva, and T. Novozhilov, Prz. Elektrotech. **9**, 157–159 (2014).
8. A. N. Novozhilov, T. A. Novozhilov, and D. M. Rakhimberdinova, Russ. Electr. Eng. **91** (6), 403–407 (2020).
9. A. N. Novozhilov, T. A. Novozhilov, E. M. Volgina, E. N. Kolesnikov, and D. M. Rakhimberdinova, Russ. Eng. Res. **40** (9), 710–713 (2020).
10. E. Volgina, A. Novozhilov, Y. Kolesnikov, D. Rahimberdinova, T. Novozhilov, and O. Andreeva, News of the National Academy of Sci. of the Rep. of Kaz., Ser. of Geology and Tech. Sci. **5** (437), 26–33 (2019).
11. A. Sarinova and A. Zamyatin. E3s Web Conf. **149**, 02003 (2020).
12. S. Kudubayeva, N. Amangeldy, A. Sundetbayeva, and A. Sarinova, Acm Int. Conf. Proc. Ser. **8**, 1–6 (2019).
13. S. Abimuldina, A. Sarinova, L. Sarlybayeva, and N. Akhmetova, Dyna **84** (202), 289–294 (2017).
14. A. Sarinova, A. Zamyatin, and P. Cabral, Dyna **82** (190), 166–172 (2015).